Orthogonally-spin-adapted coupled-cluster theory for closed-shell systems including triexcited clusters

B. G. Adams and J. Paldus*

Quantum Theory Group, Department of Applied Mathematics, University of Waterloo, Waterloo, Ontario N2L 3G1, Canada

(Received 20 November 1978)

The orthogonally-spin-adapted form of the nonlinear system of equations for the extended coupled-pair many-electron theory, which involves the monoexcited, biexcited, and triexcited states and cluster components, is derived. A diagrammatic approach, based on second quantization, the time-independent Wick theorem, and the graphical methods of spin algebras, is employed. The advantages of using the orthogonally-spin-adapted states and cluster components, rather than the nonorthogonally-spin-adapted ones which have been previously employed, particularly in the triexcited case, are also discussed. It is also shown that the formulas for the direct configuration-interaction method can easily be obtained in compact form from the linear part of the system of extended coupled-pair equations.

I. INTRODUCTION

We have recently shown[1] how the diagrammatic techniques of spin algebras[2-9] can be used to obtain an orthogonally-spin-adapted form of the coupled-cluster many-electron theory[10,11] (CCMET). The method was illustrated on the coupled-pair approach (CPMET) and the orthogonally-spin-adapted form of CPMET was given.[1]

By the orthogonally-spin-adapted form of the coupled-cluster theory we understand a form in which the connected-cluster components of the wave function are represented by *orthogonal*- (and thus linearly independent) spin-adapted N-electron configurations.[12] This is achieved by defining the appropriate linear combinations of the orbital cluster components (i.e., t_i matrix elements), and by projecting the Schrödinger equation onto the one-dimensional subspaces spanned by the corresponding *orthogonal*-spin-adapted N-electron configurations. This is particularly important when higher than biexcited clusters are considered: while the number of orbital t_2 matrix elements is the same as the number of linearly independent singlet configurations, this is not the case for higher than biexcited states.[1,11] However, even in the CPMET case, where only pair excitations are considered, the biexcited N-electron configurations associated with the orbital t_2 matrix elements are not orthogonal. In fact it can be shown that the pertinent biexcited configurations are spin-bonded functions.[13] On the other hand, the configurations used in the orthogonally-spin-adapted form of the theory are the particle-particle–hole-hole (pp-hh) coupled-spin-adapted states, which may be regarded as electronic Gelfand states (or equivalently, Yamanouchi-Kotani states)[14] of the hole-particle formalism.

Thus, in the case of triexcited clusters, there are six (three, two) distinct orbital t_3 matrix elements, but only five (two, one) linearly independent singlet configurations can be constructed. This introduces complications in the coupled-cluster approach that we have indicated earlier[11]: either one additional equation must be added for each distinct orbital occupancy or the linearly dependent t_3 matrix elements must be eliminated from the equations. The first remedy unnecessarily increases the number of equations of the system while the second leads to a highly nonsymmetric form of the equations.

In contrast, the orthogonally-spin-adapted version yields the correct number of equations for the minimal number of t_3 matrix elements needed. Moreover, the pertinent t_i matrix elements directly represent (up to possibly a simple normalization factor) the coefficients of the wave function expressed in terms of the orthonormal-spin-adapted configurations. Consequently, our formulas can easily be modified for use in the direct configuration-interaction (CI) approach of Roos and Siegbahn[15] for the triexcited configurations relative to a closed-shell ground state (cf. Ref. 4, where the corresponding expressions for the biexcited direct CI are given in terms of pp-hh coupled states).

An additional advantage of the orthogonally-spin-adapted form of the coupled pair approach is that it yields even sparser matrices for the nonlinear part of the CPMET equations. For example, in the 169-dimensional problem for the Be atom $(6s, 5p, 4d, 3f, 3g)$, the nonlinear matrices contain 3.4% nonvanishing matrix elements as compared with 4.2% in the spin-nonadapted approach.[16]

The most important contribution to the correlation energy arises from the pair clusters (biexcited cluster components), which already contribute in the second order of perturbation theory (the first order for the wave function). In the next

(i.e., third) order of perturbation theory (second order for the wave function), we find contributions from connected monoexcited and triexcited clusters as well as from the disconnected tetraexcited ones (cf. Table II of Ref. 17). The importance of these clusters is roughly proportional to their number: the largest energy contribution comes invariably from the disconnected tetraexcited clusters, while the smallest effect is due to the monoexcited ones (assuming that one starts from the Hartree-Fock orbitals).

The effect of the most essential contributions, namely, the connected biexcited and disconnected tetraexcited clusters, is accounted for in CPMET. It is also easy to include the effect of monoexcited clusters, since their number is small. However, the connected triexcited clusters require both an essential expansion of the formalism as well as a considerable increase in computational effort. Consequently, the triexcited clusters are usually neglected heuristically in both coupled-cluster and direct CI approaches.

As far as we know there have been only two coupled-cluster calculations which explicitly consider triexcited clusters: a minimal basis set *ab initio* study of the BH_3 molecule,[11] where the results were compared with the corresponding CI calculations,[18] and our recent calculations on the Be atom.[16] The BH_3 study showed quite unambiguously that in contrast to the tetraexcited clusters, where the disconnected part predominates, the major contribution in the triexcited case is due to the connected clusters, while the disconnected ones (which contribute for the first time in the next order of perturbation theory), are negligible.

We can also judge the relative importance of the triexcited and tetraexcited clusters from the results of CI calculations (knowing that in the first case these are connected clusters and in the second case the disconnected ones, which are essential in the corresponding coupled-cluster approach). Unfortunately, the triexcited states and particularly the tetraexcited ones, are very difficult to take care of in CI approaches and consequently there have been few calculations which consider these states.[19] Nevertheless, it is quite clear from several existing studies that the triexcited states may play quite an essential role in some cases and will always be important if accurate results are desired. Thus, for example, the triexcited states seem to play an important role in intermolecular (interatomic) forces, particularly in the case of the He_2 system.[20, 21] Very recently, the essential role of triexcited states was found in a study of the N_2 molecule by Ruedenberg *et al.*[22] Finally, even when the triexcited

clusters are relatively unimportant in energy calculations (less than 1% of the correlation energy), they may be important in the calculation of properties other than the energy, as is the case for the monoexcited clusters.

In this paper we present the orthogonally-spin-adapted form of the extended CPMET (ECPMET) equations. As noted above, they are also applicable to the direct CI method (after a simple renormalization and the inclusion of an unlinked diagram which does not occur in ECPMET, cf. Sec. V). It is quite remarkable that the equations involving the triexcited cluster components have a simple structure when the appropriate spin-coupling scheme is used, and the pertinent spin-coupling coefficients are all expressible in terms of one special $6\text{-}j$ symbol, which in turn is simply related to representations of the symmetric group S_3.

II. COUPLED-CLUSTER FORMALISM

To fix the notation we briefly review the formalism of the coupled-cluster theory for closed shell systems, and two of its most important approximations: the coupled-pair approach (CPMET) and an extended CPMET, referred to as ECPMET.

Consider the ground state $|\Psi\rangle$ of an $N(=2n)$ electron closed-shell system, described by a spin-independent Hamiltonian

$$H = \sum_{AB} \langle A|z|B\rangle X_A^\dagger X_B$$

$$+ \frac{1}{2} \sum_{ABCD} \langle AB|v|CD\rangle X_A^\dagger X_B^\dagger X_D X_C. \qquad (2.1)$$

The annihilation (creation) operators $X_A(X_A^\dagger)$ are defined with respect to some one-electron spin-orbital basis $\{|A\rangle\}$ where $|A\rangle = |a\rangle|\alpha\rangle$. Generally we follow the notation of Refs. 1 and 4. Thus, upper (lower) case Latin letters label spin orbitals (orbitals), lower case Greek letters label spin functions and superscripts (subscripts) designate particle (hole) states. Labels without indices [e.g., those in (2.1)] are then used to denote arbitrary one-electron functions.

In the closed-shell coupled-cluster approach the exact (nonrelativistic) ground-state wave function is expressed in the form of a cluster expansion

$$|\Psi\rangle = e^T|\Phi_0\rangle , \quad \langle\Phi_0|\Psi\rangle = \langle\Phi_0|\Phi_0\rangle = 1 , \qquad (2.2)$$

where $|\Phi_0\rangle$ is the nondegenerate independent-particle-model ground state.

The operator T has the form

$$T = \sum_{i=1}^{N} T_i , \qquad (2.3)$$

where T_i is an excitation operator creating from

$|\Phi_0\rangle$ the connected i-times excited cluster component of $|\Psi\rangle$:

$$T_i = (i!)^{-1} \sum_{\{B\}} \langle B^1 \cdots B^i | t_i | B_1 \cdots B_i \rangle \prod_{j=1}^{i} X_{B^j}^\dagger X_{B_j}$$

(2.4)

$$= (i!)^{-2} \sum_{\{B\}} \langle B^1 \cdots B^i | t_i | B_1 \cdots B_i \rangle_A \prod_{j=1}^{i} X_{B^j}^\dagger X_{B_j} ,$$

(2.5)

where $\{B\}$ denotes the unrestricted summation over all particle and hole labels specified in the t_i matrix elements. The antisymmetrized t_i matrix elements (cluster coefficients) are defined by

$$\langle B^1 \cdots B^i | t_i | B_1 \cdots B_i \rangle_A$$

$$= \sum_{P_j} (-1)^{p_j} \langle B^1 \cdots B^i | t_i | B_{j_1} \cdots B_{j_i} \rangle ,$$

(2.6)

where p_j is the parity of the permutation

$$P_j = \begin{pmatrix} 1 \cdots i \\ j_1 \cdots j_i \end{pmatrix} .$$

(2.7)

Since our Hamiltonian is spin independent, the ordinary t_i matrix elements in (2.4) can be expressed in terms of orbital t_i matrix elements[10, 12]

$$\langle B^1 \cdots B^i | t_i | B_1 \cdots B_i \rangle$$

$$= \left(\prod_{j=1}^{i} \langle \beta^j | \beta_j \rangle \right) \langle b^1 \cdots b^i | t_i | b_1 \cdots b_i \rangle .$$

(2.8)

The t_i matrix elements also possess the symmetry properties

$$\langle B^{k_1} \cdots B^{k_i} | t_i | B_{k_1} \cdots B_{k_i} \rangle$$

$$= \langle B^1 \cdots B^i | t_i | B_1 \cdots B_i \rangle ,$$

(2.9)

$$\langle B^{k_1} \cdots B^{k_i} | t_i | B_{j_1} \cdots B_{j_i} \rangle_A$$

$$= (-1)^{p_k + p_j} \langle B^1 \cdots B^i | t_i | B_1 \cdots B_i \rangle_A ,$$

(2.10)

and we note that (2.9) is also satisfied by the orbital t_i matrix elements defined in (2.8).

In order to obtain the explicit form of the coupled-cluster equations, using the diagrammatic methods based on the generalized time-independent Wick theorem,[23] it is convenient to use the normal product form of the Schrödinger equation[10, 23]

$$H_N | \Psi \rangle = \Delta\epsilon | \Psi \rangle ,$$

(2.11)

where

$$H_N = H - \langle \Phi_0 | H | \Phi_0 \rangle = F_N + V_N ,$$

(2.12)

$$F_N = \sum_{AB} \langle A | f | B \rangle N[X_A^\dagger X_B] ,$$

(2.13)

$$V_N = \frac{1}{2} \sum_{ABCD} \langle AB | v | CD \rangle N[X_A^\dagger X_B^\dagger X_D X_C] ,$$

(2.14)

and the correlation energy $\Delta\epsilon$ is defined by

$$\Delta\epsilon = E - \langle \Phi_0 | H | \Phi_0 \rangle ,$$

(2.15)

where E is the exact ground-state energy eigenvalue of H. The one-electron matrix elements in (2.13) are given by

$$\langle A | f | B \rangle = \langle A | z | B \rangle + \sum_{C_1} \langle AC_1 | v | BC_1 \rangle_A ,$$

(2.16)

where

$$\langle AB | v | CD \rangle_A = \langle AB | v | CD \rangle - \langle AB | v | DC \rangle .$$

(2.17)

If the reference state $|\Phi_0\rangle$ is chosen as the Hartree-Fock (HF) wave function, then f is just the one-electron HF operator.

The Schrödinger equation (2.11) can be cast into the form

$$(H_N e^T)_C | \Phi_0 \rangle = \Delta\epsilon | \Phi_0 \rangle ,$$

(2.18)

where the subscript C refers to the connected resulting diagrams formed from one H skeleton and one M skeleton (collection of T skeletons).[10, 11] This is the basic equation of the coupled-cluster theory and is completely equivalent to the original Schrödinger equation (2.11).

By projecting (2.18) onto the one-dimensional subspaces, defined by the appropriate set of linearly independent N-electron configurations, we obtain a system of coupled nonlinear algebraic equations, determining the various t_i matrix elements. The subset of these equations corresponding to projections onto the subspace of i-times excited configurations is obtained from the connected resulting diagrams having i open paths. It is important to realize that the system of coupled-cluster equations does not contain the correlation energy and that this follows quite naturally from the diagrammatic approach. In fact, the correlation energy is determined in terms of only the t_1- and t_2-matrix elements via a separate equation

$$\Delta\epsilon = \langle \Phi_0 | (H_N e^T)_C | \Phi_0 \rangle ,$$

(2.19)

obtained by projecting (2.18) onto $|\Phi_0\rangle$, or equivalently from the connected resulting diagrams having no open paths (no external lines).

In practice the system of coupled-cluster equations must be truncated by including in the expansion (2.2) of the exact wave function only the most important clusters, and projecting (2.18) onto the pertinent finite dimensional subspaces.

In CPMET the following approximation is used:

$$T \simeq T_2 ,$$

(2.20)

and (2.18) is projected onto the subspace spanned by the biexcited configurations. This is a useful approximation whenever the connected tetraexcited cluster component T_4 is negligible compared to the disconnected component $\frac{1}{2}T_2^2$. We recall that while the disconnected component appears for the first time in the second order of perturbation theory, the connected component appears for the first time in third order.

This situation is reversed for the triexcited component: the connected component T_3 appears in second order, whereas the disconnected components first appear in the third order. This leads to a version of ECPMET defined by

$$T \simeq T_1 + T_2 + T_3 . \tag{2.21}$$

In the expansion of $\exp(T)$ we then keep the linear terms T_1, T_2, and T_3 and the nonlinear term $\frac{1}{2}T_2^2$, which take into account all clusters appearing in the first two orders of perturbation theory and we neglect all other disconnected terms, such as $\frac{1}{2}T_1^2$, $(1/3!)T_1^3$, $T_1 T_2$, etc., appearing for the first time in higher orders (cf. Table II of Ref. 17). In this case we project Eq. (2.18) onto the subspaces determined by the appropriate monoexcited, biexcited, and triexcited configurations.

The spin-orbital form of the coupled-cluster theory[10, 11] is obtained by projecting Eq. (2.18) onto the i-times excited configurations ($i = 1, 2, \ldots$)

$$\left| \begin{matrix} A^1 \cdots A^i \\ A_1 \cdots A_i \end{matrix} \right\rangle = \left(\prod_{j=1}^{i} X^{\dagger}_{A^j} X_{A_j} \right) | \Phi_0 \rangle . \tag{2.22}$$

In this case three types of diagrams may be used to obtain the resulting system of equations: Hugenholtz diagrams[10] (antisymmetrized t and v matrix elements), Goldstone diagrams (ordinary t and v matrix elements), and the mixed Goldstone-Hugenholtz[1] (Brandow[24]) diagrams (ordinary v and antisymmetrized t-matrix elements).

For the spin-independent Hamiltonians, which we are considering, an orbital form of the coupled-cluster equations may be obtained from the Goldstone version of the spin-orbital form by summing over all spin-projection quantum numbers, and using (2.8) and the spin independence of the f and v matrix elements to obtain a system of equations involving the orbital t, f, and v matrix elements. This is most easily achieved by assigning a factor of 2 to each closed loop of the Goldstone diagrams, and replacing all spin-orbital matrix elements by their corresponding orbital ones. We shall refer to these equations as nonorthogonally-spin-adapted equations,[12] since they do not correspond to projections of the Schrödinger equation (2.18) onto an *orthonormal*

set of configurations, but rather to projections onto a *nonorthogonal* set of spin-bonded functions.[13]

In contrast, by an orthogonally-spin-adapted form of the coupled-cluster theory, we mean one for which the Schrödinger equation (2.18) is projected onto an orthonormal set of spin-adapted configurations.

A convenient procedure for obtaining the explicit form of the orthogonally spin adapted coupled cluster equations has been formulated in Ref. 1, using the Goldstone-Hugenholtz orbital diagrams in Brandow form (Goldstone v and f vertices and Brandow t vertices), which were referred to as Goldstone-Brandow diagrams. The rules for the assignment of f and v matrix elements to the Goldstone one- and two-electron interaction vertices, spin-adapted t_i matrix elements to the Brandow vertices, the evaluation of sign and weight factors, and the construction of the spin diagram associated with each orbital diagram are also given in Ref. 1. We would also like to mention that a similar approach to atomic systems, using spin and orbital angular-momentum diagrams, and based on the Goldstone formalism, has been recently given.[7]

III. SPIN-ADAPTED STATES AND CLUSTER COMPONENTS

We now construct the orthonormal-spin-adapted monoexcited, biexcited, and triexcited configuration states and discuss their symmetry properties. It is shown that the recoupling transformations, which are needed for the triexcited states, are simply related to representation matrices of the symmetric group S_3. The spin adaptation and the recoupling transformations can easily be obtained by using the graphical methods of spin algebras, which we have previously applied to the orthogonally spin adapted CPMET approach,[1] to the derivation of compact formulas for spin adapted CI matrix elements between biexcited states,[4, 25] and very recently to obtain the matrix elements for Serber states.[26] Finally, the spin-adapted t_1, t_2, and t_3 matrix elements are constructed in the same manner as the corresponding states. In this way, for each fixed orbital occupancy, we obtain a one-to-one correspondence between the orthogonal (and thus linearly independent) spin-adapted states and the distinct t_3 matrix elements. As a result, in the orthogonally-spin-adapted coupled-cluster equations, there will always be the same number of equations as there are distinct t matrix elements

A. Orthogonal-spin-adapted states

The orthogonal-spin-adapted states are constructed from the basic spin-orbital configurations.

$$\begin{vmatrix} B^1 \cdots B^i \\ B_1 \cdots B_i \end{vmatrix} = \begin{vmatrix} b^1\beta^1 \cdots b^i\beta^i \\ b_1\beta_1 \cdots b_i\beta_i \end{vmatrix} = \left(\prod_{j=1}^{i} X_{B^j}^\dagger X_{B_j} \right) |\Phi_0\rangle .$$

$$(3.1)$$

We have shown earlier[4] that it is more convenient, in the hole-particle formalism, to use the configurations

$$\begin{bmatrix} B^1 \cdots B^i \\ B_1 \cdots B_i \end{bmatrix} = \left(\prod_{j=1}^{i} (-1)^{s_j - \beta_j} \right) \begin{vmatrix} b^1\beta^1 \cdots b^i\beta^i \\ b_1\bar\beta_1 \cdots b_i\bar\beta_i \end{vmatrix} ,$$

$$(3.2)$$

where $\bar\beta = -\beta$ and $s_j = \frac{1}{2}$ ($j = 1, \ldots, i$). These configurations can be coupled in the usual way to obtain the spin-adapted states

$$\begin{vmatrix} b^1 \cdots b^i \\ b_1 \cdots b_i \end{vmatrix} SM \rangle^{X^S}_{X_S}$$

$$= N_b \sum_{\{\beta\}} [X_S X^S \{\beta\} SM] \begin{bmatrix} b^1\beta^1 \cdots b^i \beta^i \\ b_1\beta_1 \cdots b_i \beta_i \end{bmatrix} \qquad (3.3a)$$

$$= N_b \sum_{\{\beta\}} \langle X_S X^S \{\beta\} SM| \begin{vmatrix} b^1\beta^1 \cdots b^i \beta^i \\ b_1\beta_1 \cdots b_i \beta_i \end{vmatrix} . \qquad (3.3b)$$

The coefficient in (3.3a) is a generalized Clebsch-Gordan coefficient (CG), defined by the chosen coupling scheme, and given as a product of the ordinary CG coefficients of SU(2). Further, X_S and X^S are the sets of intermediate spin quantum numbers for the hole- and particle-coupling schemes, respectively, S and M are the total spin and spin-projection quantum numbers, $\{\beta\}$ denotes summation over all spin-projection quantum numbers except M, and N_b is a normalization factor. Other coupling schemes are possible, namely, those which include hole-particle couplings. However, they give rise to more complicated formulas, symmetry properties and spin diagrams (cf., for example Ref. 4, where both the pp-hh and ph-ph coupling schemes were considered for biexcited states). The transition from (3.3a) to (3.3b) is easily made by using the well-known symmetry properties of the CG coefficients.[8]

If we sequentially couple the hole (particle) states and define

$$C_2 = \langle s_2\beta_2 s_1\beta_1 | S_{12}\beta_{12} \rangle \langle s^1\beta^1 s^2\beta^2 | S^{12}\beta^{12} \rangle , \qquad (3.4a)$$

$$C_3 = \langle s_1\beta_1 s_2\beta_2 | S_{12}\beta_{12} \rangle \langle s^1\beta^1 s^2\beta^2 | S^{12}\beta^{12} \rangle$$

$$\times \langle S_{12}\beta_{12} s_3\beta_3 | S_{123}\beta_{123} \rangle \langle S^{12}\beta^{12} s^3\beta^3 | S^{123}\beta^{123} \rangle ; \qquad (3.4b)$$

then the coefficients in (3.3a) for the monoexcited, biexcited, and triexcited states are given by

$$[\{\beta\} SM] = \langle s_1\beta_1 s^1\beta^1 | SM \rangle , \qquad (3.5a)$$

$$[S_{12}S^{12}\{\beta\} SM] = C_2 \langle S_{12}\beta_{12} S^{12}\beta^{12} | SM \rangle , \qquad (3.5b)$$

$$[S_{12}S_{123}S^{12}S^{123}\{\beta\} SM] = C_3 \langle S_{123}\beta_{123} S^{123}\beta^{123} | SM \rangle , \qquad (3.5c)$$

and hence those in (3.3b) are given by

$$\langle \{\beta\} SM \rangle = (\tfrac{1}{2}[S])^{1/2} \langle SM s_1\beta_1 | s^1\beta^1 \rangle , \qquad (3.6a)$$

$$\langle S_{12}S^{12}\{\beta\} SM \rangle = C_2([S]/[S^{12}])^{1/2} \times \langle SM S_{12}\beta_{12} | S^{12}\beta^{12} \rangle , \qquad (3.6b)$$

$$\langle S_{12}S_{123}S^{12}S^{123}\{\beta\} SM \rangle = C_3([S]/[S^{123}])^{1/2} \times \langle SM S_{123}\beta_{123} | S^{123}\beta^{123} \rangle , \qquad (3.6c)$$

where we have used the shorthand notation

$$[X] \equiv 2X + 1 . \qquad (3.7)$$

Thus, the monoexcited, biexcited, and triexcited states, which we shall use, are

$$\begin{vmatrix} b^1 \\ b_1 \end{vmatrix} SM \rangle = \sum_{\{\beta\}} \langle \{\beta\} SM \rangle \begin{vmatrix} b^1\beta^1 \\ b_1\beta_1 \end{vmatrix} , \qquad (3.8a)$$

$$\begin{vmatrix} b^1 b^2 \\ b_1 b_2 \end{vmatrix} SM \rangle^{S^{12}}_{S_{12}} = N_b \sum_{\{\beta\}} \langle S_{12}S^{12}\{\beta\} SM \rangle \begin{vmatrix} b^1\beta^1 b^2\beta^2 \\ b_1\beta_1 b_2\beta_2 \end{vmatrix} , \qquad (3.8b)$$

$$\begin{vmatrix} b^1 b^2 b^3 \\ b_1 b_2 b_3 \end{vmatrix} SM \rangle^{S^{12}S^{123}}_{S_{12}S_{123}} = N_b \sum_{\{\beta\}} \langle S_{12}S_{123}S^{12}S^{123}\{\beta\} SM \rangle$$

$$\times \begin{vmatrix} b^1\beta^1 b^2\beta^2 b^3\beta^3 \\ b_1\beta_1 b_2\beta_2 b_3\beta_3 \end{vmatrix} . \qquad (3.8c)$$

Since we are considering closed-shell systems, only the singlets ($S = M = 0$) are needed, and we introduce the simplified notations

$$\begin{vmatrix} b^1 \\ b_1 \end{vmatrix} \rangle \equiv \begin{vmatrix} b^1 \\ b_1 \end{vmatrix} 00 \rangle , \qquad (3.9a)$$

$$\begin{vmatrix} b^1 b^2 \\ b_1 b_2 \end{vmatrix} S_i \rangle \equiv \begin{vmatrix} b^1 b^2 \\ b_1 b_2 \end{vmatrix} 00 \rangle^{S_i} \quad (S_i = S_{12} = S^{12}) , \qquad (3.9b)$$

$$\begin{vmatrix} b^1 b^2 b^3 \\ b_1 b_2 b_3 \end{vmatrix} S \rangle \equiv \begin{vmatrix} b^1 b^2 b^3 \\ b_1 b_2 b_3 \end{vmatrix} 00 \rangle^{S^{12}S_I}_{S_{12}S_I} \quad (S_I = S_{123} = S^{123}) , \qquad (3.9c)$$

where $\mathcal{S} = \{S_{12}, S^{12}, S_I\}$ is the set of intermediate-spin quantum numbers for the triexcited singlet states. We shall also omit the b labels, if no confusion can arise, and simply indicate the appropriate subscripts and superscripts within the "bra" or "ket" symbols. Thus, we shall write, for example

$$\left| \begin{matrix} i\ j\ k \\ l\ m\ n \end{matrix}\ \mathcal{S} \right\rangle \equiv \left| \begin{matrix} b^i\ b^j\ b^k \\ b_l\ b_m b_n \end{matrix}\ \mathcal{S} \right\rangle . \qquad (3.10)$$

For the biexcited states in (3.8b) or (3.9b), the normalization factor is simply given by

$$N_b = \left\{ [\ 1 + \delta(b_1, b_2)][\ 1 + \delta(b^1, b^2)] \right\}^{-1/2} . \qquad (3.11)$$

For the triexcited states, Eq. (3.9c), the same normalization factor can be used if we make the *standard ordering convention*, namely, that a doubly occupied particle (or hole) orbital always appears in the first two particle (or hole) positions in (3.9c).[27] This can always be achieved by a simple recoupling transformation [cf. Eq. (3.17)].

B. Graphical representation

As mentioned earlier, it is most convenient to use the mixed Goldstone-Hugenholtz (or Brandow) representation (cf. Refs. 1 and 24). Thus, for the orbital diagrams we use one Goldstone representative of the Hugenholtz diagram for our states

and the Goldstone representation for the spin-independent one- and two-electron operators of the Hamiltonian. The spin part will then be represented by the usual angular-momentum diagrams (cf. Refs. 1, 3, and 4).

Thus, the orbital diagrams for the states will have the form shown in Fig. 11(a) of Ref. 1. The corresponding spin diagrams are most easily constructed using CG vertices. They can be subsequently transformed to a more symmetric form in terms of 3-jm vertices, using the transformation rules (64a and 64b) of Ref. 4. The spin diagrams for the monoexcited and biexcited states (3.8a) and (3.8b), have been given in Fig. 2 of Ref. 4. The singlet case (3.9b) has also been given in Fig. 4 of Ref. 1. Here we give only the spin diagrams for the triexcited states (3.9c) in Fig. 1, using 3-jm vertices. For the sake of brevity, we also introduce a more compact form for these diagrams which is shown in Figs. 1(b) and 1(d).

C. Symmetry properties of spin-adapted states

We now consider the symmetry properties of the orthogonally-spin-adapted states (3.9). For the biexcited states we obtain the simple symmetry property

$$\left| \begin{matrix} \bar{\tau}\ \tau \\ \bar{\mu}\ \mu \end{matrix}\ S_i \right\rangle = (-1)^{(\tau+\mu)\,s_i} \left| \begin{matrix} 1\ 2 \\ 1\ 2 \end{matrix}\ S_i \right\rangle , \qquad (3.12)$$
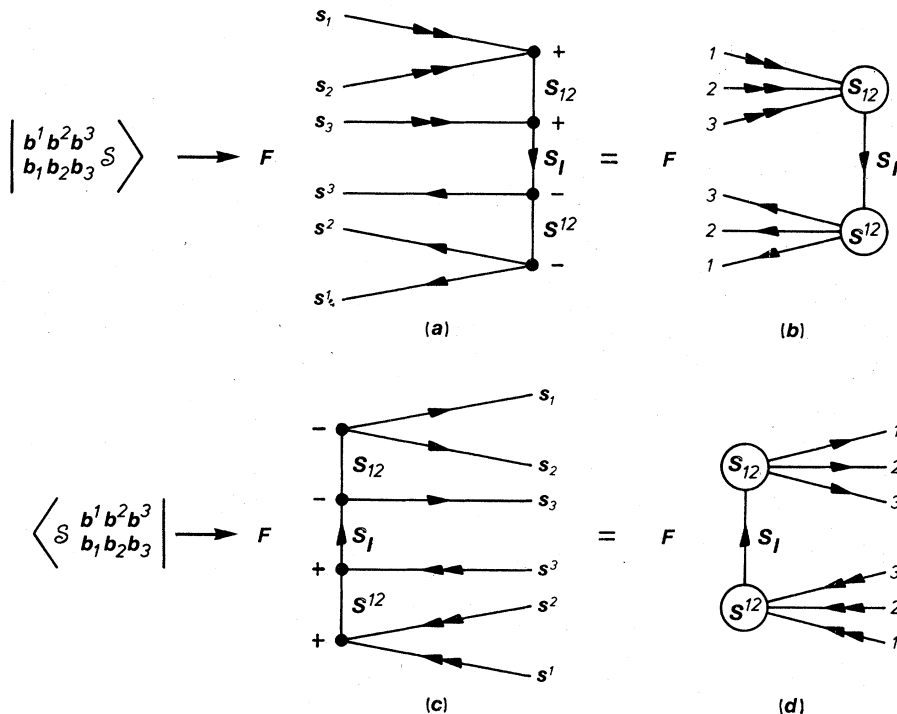

FIG. 1. Graphical representation of the spin parts of the spin-adapted triexcited "ket" states (a) and (b) and "bra" states (c) and (d). The overall factor for each diagram is $F = (-1)\ [S_{12}, S^{12}, S_I]^{1/2}$ and $s_j = s^j = \frac{1}{2}$, $j = 1, 2, 3$. Diagrams (a) or (b) also represent the spin parts of the t_3 matrix elements associated with the Brandow t_3 vertices of Figs. 3 and 4.

where

$$\tau, \mu = 1, 2 \quad (\bar{1} = 2, \bar{2} = 1) .$$ (3.13)

If the particle and/or hole states are doubly occupied, it then follows that

$$\left|\begin{matrix} 1 & 1 \\ 1 & 2 \end{matrix} \; 1\right\rangle = \left|\begin{matrix} 1 & 2 \\ 1 & 1 \end{matrix} \; 1\right\rangle = \left|\begin{matrix} 1 & 1 \\ 1 & 1 \end{matrix} \; 1\right\rangle = 0 .$$ (3.14)

For the triexcited singlet states, the corresponding results are more complicated, except for transpositions of the first pair of particle and/or hole states:

$$\left|\begin{matrix} \bar{\tau} & \tau & 3 \\ \bar{\mu} & \mu & 3 \end{matrix} \; S\right\rangle = (-1)^{\tau S^{12} + \mu S_{12}} \left|\begin{matrix} 1 & 2 & 3 \\ 1 & 2 & 3 \end{matrix} \; S\right\rangle ,$$ (3.15)

which is identical to the corresponding results for the biexcited states in (3.8b) [cf. Eqs. (29) of Ref. 4]. For more general permutations, we must consider the recoupling transformation

$$\left|\begin{matrix} k_1 k_2 k_3 \\ j_1 j_2 j_3 \end{matrix} \; S\right\rangle = \sum_{\tilde{S}} \left|\begin{matrix} 1 & 2 & 3 \\ 1 & 2 & 3 \end{matrix} \; \tilde{S}\right\rangle \left\langle\begin{matrix} 1 & 2 & 3 \\ 1 & 2 & 3 \end{matrix} \; \tilde{S} \middle| \begin{matrix} k_1 k_2 k_3 \\ j_1 j_2 j_3 \end{matrix} \; S\right\rangle ,$$

(3.16)

corresponding to the permutations P_k and P_j of the particle- and hole-state indices, respectively [cf. Eq. (2.7)]. In (3.16), $S = \{S_{12}, S^{12}, S_I\}$ and $\tilde{S} = \{\tilde{S}_{12}, \tilde{S}^{12}, \tilde{S}_I\}$. In general, the recoupling transformation matrix in (3.16) is the product of an

orbital phase factor $(-1)^{p_k + p_j}$, determined by the parities of these permutations (and follows from the resulting orbital diagram), and a spin coefficient given by the resulting spin diagram. The latter is obtained by connecting the pertinent lines of the "ket"-state spin diagram of Fig. 1(a) to the lines of the "bra"-state spin diagram of Fig. 1(c), as determined by the orbital diagram (or, equivalently, by the permutations P_k and P_j). Thus, for example, the "ket"-state line with label s^{k_1} is connected to the "bra"-state line with label s^1. The resulting spin diagram, giving the spin part of the recoupling transformation matrix, is shown in Fig. 2, where we have taken into account all 36 possibilities using the indices τ, μ defined in (3.13) and the indices κ, $\lambda = 1, 2, 3$. Each particle or hole index is evaluated modulo 3 (i.e., $4 = 1$, $5 = 2$, $6 = 3$). Thus, the identity permutation corresponds to $\kappa = \lambda = 3$, $\tau = 2$ and the special case given in (3.15) corresponds to $\kappa = \lambda = 3$. This notation is very convenient for computer implementation of the ECPMET equations (cf. Sec. IV). Using the graphical rules of spin algebras (cf. Appendix I of Ref. 4 for a useful summary) this spin diagram can be separated across two lines (S_I and $\tilde{S}_I$) and the summation over $\tilde{S}_I$ in (3.16) disappears [rule (70) of Ref. 4]. Each of the two resulting component spin diagrams is proportional to either a Kronecker delta [$\delta(S_{12}, \tilde{S}_{12})$ or $\delta(S^{12}, \tilde{S}^{12})$] or a simple 6-$j$ symbol with three angular momenta equal to one-half. Thus, the most complicated spin coefficient is proportional to a product of two 6-j sym-
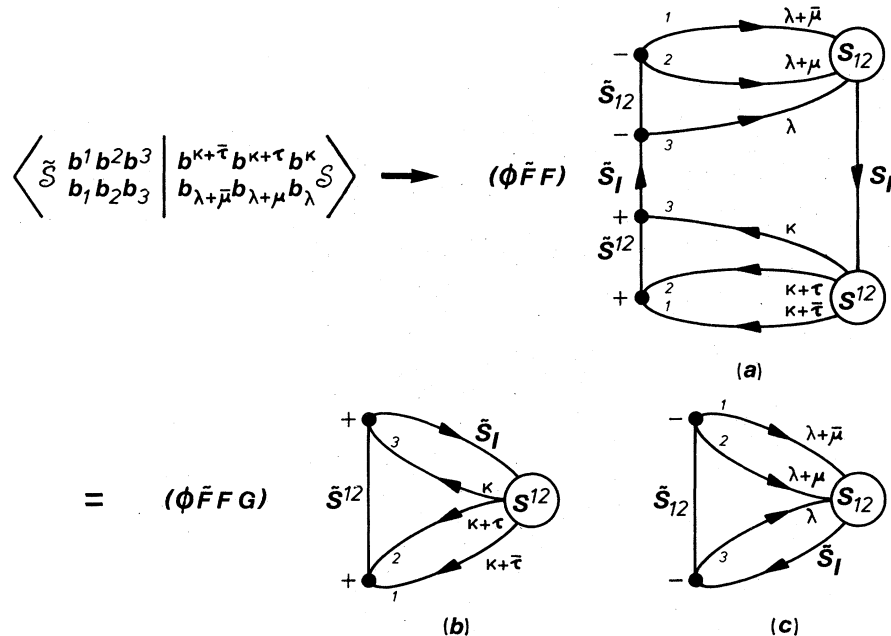

FIG. 2. Graphical calculation of overlap matrix element between two triexcited states (cf. text for details). The overall factors are defined by $\phi = (-1)^{\tau + \mu}$, $F = (-1) [S_{12}, S^{12}, S_I]^{1/2}$, and $G = [\tilde{S}_I]^{-1} \times \delta(\tilde{S}_I, S_I)$, where ϕ is the orbital phase factor [cf. remarks following (3.16) of text]. Diagrams (b) and (c), along with the factors $\tilde{F}$, F, G, give the spin coefficients (3.18) that appear in (3.17).

TABLE I. Spin coefficient defined in Eqs. (3.18) and (3.19) (cf. also Table II).

κ	$D_\kappa(Z;X,Y)$
1	$(-1)^Y\Delta(Z;X,Y)$
2	$(-1)^X\Delta(Z;X,Y)$
3	$\delta(X,Y)$

bols, and (3.16) can be written in the compact form

$$\begin{vmatrix} \kappa+\bar{\tau} & \kappa+\tau & \kappa \\ \lambda+\bar{\mu} & \lambda+\mu & \lambda \end{vmatrix} S \Bigg\rangle = \sum_{\tilde{S}} (-1)^{\tau+\mu} D_{\kappa,\tau}(S_I;S^{12},\tilde{S}^{12})$$

$$\times D_{\lambda,\mu}(S_I;S_{12},\tilde{S}_{12})\delta(S_I,\tilde{S}_I)$$

$$\times \begin{vmatrix} 1\ 2\ 3 \\ 1\ 2\ 3 \end{vmatrix} \tilde{S} \Bigg\rangle, \qquad (3.17)$$

where

$$D_{\kappa,\tau}(Z;X,Y) = (-1)^{\tau(1+Y)} D_\kappa(Z;X,Y), \quad (3.18)$$

and D_κ is defined in Table I in terms of

$$\Delta(Z;X,Y) = \Delta(Z;Y,X) = [X,Y]^{1/2} \begin{Bmatrix} \frac{1}{2} & Z & X \\ \frac{1}{2} & \frac{1}{2} & Y \end{Bmatrix}. \qquad (3.19)$$

Here we are using a generalization of the notation in (3.7), namely,

$$[X_1,X_2,\dots,X_n] = [X_1][X_2]\dots[X_n]. \qquad (3.20)$$

The possible values of $\Delta(Z;X,Y)$ are given in Table II.

It is worth noting in (3.17) that $(-1)^{\tau+\mu}$ is just the orbital phase factor mentioned above. Further, if we define

$$\Phi_\tau(X,Y) = (-1)^{\tau Y}\delta(X,Y); \quad \tau = 1,2, \qquad (3.21)$$

then the six matrices $\Phi_\tau D_\kappa$ with $Z = \frac{1}{2}$ and with rows and columns labeled by $X,Y = 0,1$, form a two-dimensional irreducible representation of the symmetric group S_3. For $S_I = \frac{3}{2}$, we obtain the

TABLE II. Spin coefficient defined in Eq. (3.19).

X	Y	Z	$\Delta(Z,X,Y)$
0	0	$\frac{1}{2}$	$-\frac{1}{2}$
0	1	$\frac{1}{2}$	$\frac{1}{2}\sqrt{3}$
1	1	$\frac{1}{2}$	$\frac{1}{2}$
1	1	$\frac{3}{2}$	-1

one-dimensional antisymmetric representation, since $D_\kappa(\frac{3}{2}; 1,1) = 1$ is the only nonvanishing matrix element. The matrices D_κ represent cyclic permutations with the group property

$$\sum_Y D_\kappa(Z;X,Y)D_\lambda(Z;Y,X') = D_{\kappa+\lambda}(Z;X,X'), \qquad (3.22)$$

which includes as special cases the orthogonality relations[8]

$$\sum_Y \Delta(Z;X,Y)\Delta(Z;Y,X') = \delta(X,X'), \qquad (3.23)$$

satisfied by the 6-j symbols, and the Racah-Elliot sum rule[8,28]

$$\sum_Y (-1)^Y \Delta(Z;X,Y)\Delta(Z;Y,X')$$

$$= (-1)^{X+X'}\Delta(Z;X,X'). \qquad (3.24)$$

Thus, the transformation matrix in (3.17) can be interpreted as the outer direct product of two representations of S_3, one corresponding to permutations of particles, the other to permutations of holes. For $S_I = \frac{3}{2}$ we obtain the trivial recoupling transformation

$$\begin{vmatrix} \kappa+\bar{\tau} & \kappa+\tau & \kappa \\ \lambda+\bar{\mu} & \lambda+\mu & \lambda \end{vmatrix} 1,1,\frac{3}{2} \Bigg\rangle = (-1)^{\tau+\mu} \begin{vmatrix} 1\ 2\ 3 \\ 1\ 2\ 3 \end{vmatrix} 1,1,\frac{3}{2} \Bigg\rangle. \qquad (3.25)$$

Finally we note that all recoupling transformations can be obtained from those corresponding to the transpositions (12) and (13):

$$P_{12} \begin{vmatrix} 1\ 2\ 3 \\ 1\ 2\ 3 \end{vmatrix} S \Bigg\rangle \equiv \begin{vmatrix} 1\ 2\ 3 \\ 2\ 1\ 3 \end{vmatrix} S \Bigg\rangle$$

$$= (-1)^{S_{12}} \begin{vmatrix} 1\ 2\ 3 \\ 1\ 2\ 3 \end{vmatrix} S \Bigg\rangle, \qquad (3.26a)$$

$$P_{13} \begin{vmatrix} 1\ 2\ 3 \\ 1\ 2\ 3 \end{vmatrix} S \Bigg\rangle \equiv \begin{vmatrix} 1\ 2\ 3 \\ 3\ 2\ 1 \end{vmatrix} S \Bigg\rangle$$

$$= \sum_{\tilde{S}} \delta(S_I,\tilde{S}_I)\delta(S^{12},\tilde{S}^{12})$$

$$\times \Delta(S_I;S_{12},\tilde{S}_{12}) \begin{vmatrix} 1\ 2\ 3 \\ 1\ 2\ 3 \end{vmatrix} \tilde{S} \Bigg\rangle, \qquad (3.26b)$$

and the analogous results for the particle permutations.

D. Spin-adapted t_i matrix elements

To obtain the spin-adapted t_i matrix elements we first write the i-times excited connected cluster component of the wave function in the form

$$T_i| \Phi_0\rangle =\sum_{SM} T_i(SM)| \Phi_0\rangle . \qquad (3.27)$$

For closed-shell systems we need only consider the singlet components

$$T_1(00)| \Phi_0\rangle = \sum_{\{b\}}\langle b^1| t_1(0)|b_1\rangle \left|\begin{matrix} b^1 \\ b_1\end{matrix}\right\rangle, \qquad (3.28a)$$

$$T_2(00)| \Phi_0\rangle =\frac{1}{(2!)^2}\sum_{S_i}\ \sum_{\{b\}} N_b^{-2}$$

$$\times \langle b^1b^2| t_2(S_i)| b_1b_2\rangle \left|\begin{matrix} b^1b^2 \\ b_1b_2\end{matrix}\ S_i\right\rangle, (3.28b)$$

$$T_3(00)| \Phi\rangle =\frac{1}{(3!)^2}\sum_{S}\sum_{\{b\}} N_b^{-2}$$

$$\times \langle b^1b^2b^3| t_3(\mathcal{S})| b_1b_2b_3\rangle \left|\begin{matrix} b^1b^2b^3 \\ b_1b_2b_3\end{matrix}\ \mathcal{S}\right\rangle,$$

$$(3.28c)$$

where $\mathcal{S} =\{ S_{12},S^{12},S_I\}$ and $\{b\}$ denotes unrestricted summation over all orbital labels. The normalization factors ensure that each distinct state is counted only once. The spin-adapted t_1, t_2 and t_3 matrix elements are defined in the same way as the corresponding states [cf. Eqs. (3.8) and (3.9)]:

$$\langle b^1| t_1(0)| b_1\rangle =\sum_{\{\beta\}}\langle \{\beta\}00\rangle\langle b^1\beta^1|t_1| b_1\beta_1\rangle , \qquad (3.29a)$$

$$\langle b^1b^2| t_2(S_i)|b_1b_2\rangle =N_b\sum_{\{\beta\}}\langle S_i S_i\{\beta\}00\rangle$$

$$\times\langle b^1\beta^1b^2\beta^2|t_2| b_1\beta_1b_2\beta_2\rangle_A , \qquad (3.29b)$$

$$\langle b^1b^2b^3| t_3(\mathcal{S})| b_1b_2b_3\rangle =N_b\sum_{\{\beta\}}\langle S_{12}S_I S^{12}S_I\{\beta\}00\rangle$$

$$\times\langle b^1\beta^1b^2\beta^2b^3\beta^3|t_3| b_1\beta_1b_2\beta_2b_3\beta_3\rangle_A. \qquad (3.29c)$$

It follows that the spin-adapted t_i matrix elements possess exactly the same symmetry properties as the corresponding states. Thus, (3.17), (3.25), and (3.26) are also valid if the states are replaced by t matrix elements and hence we obtain, for each fixed orbital occupancy, the same number (5, 2, or 1) of spin-adapted t_3 matrix elements as spin-adapted triexcited states. This is summar-

TABLE III. Nonvanishing linearly independent triexcited states or t_3 matrix elements (cf. Sec. III for details).

X: Nonvanishing triexcited states or t_3 matrix elements						
S^{12}	S_{12}	S_I	$b^1>b^2>b^3$ $b_1>b_2>b_3$	$b^1=b^2$ $b_1=b_2$	$b^1=b^2$ $b_1=b_2$	$b^1=b^2$ $b_1=b_2$
0	0		X	X	X	X
0	1	$\frac{1}{2}$	X	X		
1	0		X		X	
1	1		X			
1	1	$\frac{3}{2}$	X			
	Totals		5	2	2	1

ized in Table III for states or matrix elements satisfying the standard ordering convention in which doubly occupied orbitals appear in the first two positions. As mentioned above, the normalization factor in (3.11) applies in this case. This is the only case that we need to consider: if a doubly occupied orbital appears in other positions, it follows from the recoupling transformations (3.17) and Table III that such states or t_3 matrix elements are simply proportional to one of the standard ordered ones. In case all orbitals are singly occupied ($N_b = 1$ in this case), the standard ordering convention may, for example, be defined by $b^1>b^2>b^3$, $b_1>b_2>b_3$ in terms of the chosen ordering of the one-electron orbitals and again the recoupling transformations may be used to express any state or t_3 matrix element as a linear combination of standard ordered ones. If particle, hole, or particle and hole recouplings are needed a linear combination of at most 2, 2, or 4 standard ordered states or matrix elements is obtained [for $S_I =\frac{3}{2}$ we always obtain a simple proportionality, Eq. (3.25)].

The spin-adapted t matrix elements can also be expressed in terms of the orbital t matrix elements of the nonorthogonally spin-adapted theory[12]

$$\langle b^1| t_1(0)| b_1\rangle =\sqrt{2}\langle b^1| t_1| b_1\rangle , \qquad (3.30a)$$

$$\langle b^1b^2| t_2(S_i)| b_1b_2\rangle$$

$$=-N_b[S_I]^{1/2}\sum_{\kappa=1}^{2}(-1)^{\kappa S_i}\langle b^1b^2| t_2| b_\kappa b_{\bar{\kappa}}\rangle, \qquad (3.30b)$$

$$\langle b^1b^2b^3| t_3(\mathcal{S})| b_1b_2b_3\rangle$$

$$=N_b[S_I]^{1/2}\sum_{\kappa=1}^{3}\sum_{\tau=1}^{2}(-1)^{\tau S_{12}}D_\kappa(S_I;S^{12},S_{12})$$

$$\times\langle b^{\kappa+\bar{\tau}}b^{\kappa+\tau}b^\kappa| t_3| b_1b_2b_3\rangle . \qquad (3.30c)$$

If desired we can avoid the normalization factors completely by defining unnormalized t_2 and t_3 matrix elements [cf. Eq. (32) of Ref. 1],

$$\langle b^1 b^2| \ \tau_2(S_i)|b_1 b_2\rangle = N_b^{-1}\langle b^1 b^2| \ t_2(S_i)b_1 b_2\rangle , \quad (3.31a)$$

$$\langle b^1 b^2 b^3| \ \tau_3(S)| \ b_1 b_2 b_3\rangle = N_b^{-1}\langle b^1 b^2 b^3| \ t_3(S)| \ b_1 b_2 b_3\rangle . \quad (3.31b)$$

Thus, if these matrix elements are used in (3.28) and unnormalized states are also used then all normalization factors are removed. The normalization factors can easily be reintroduced into the equations. They are needed to obtain the direct CI formulas (cf. Sec. V). In Sec. IV we give the spin-adapted form of the ECPMET equations using the unnormalized matrix elements.

IV. SPIN-ADAPTED ECPMET EQUATIONS

We now present the explicit form of the orthogonally-spin-adapted ECPMET equations by projecting the Schrödinger equation (2.18) onto the monoexcited, biexcited, and triexcited spin-adapted states defined in (3.9), and by using the Goldstone-Hugenholtz (Brandow) diagrams combined with the graphical methods of spin algebras to enumerate and evaluate the various contributions. For completeness the CPMET part of this system, which has been given elsewhere,[1] is also included.

We can express the left-hand side of the Schrödinger equation (2.18) as a sum of i-times excited components ($i = 0, 1, \ldots$):

$$(H_N e^T)_C \ | \ \Phi_0\rangle = \sum_{i=0}^{N} \ \mathcal{H}_C^{(i)} | \ \Phi_0\rangle . \quad (4.1)$$

If we use the ECPMET approximation (2.21), project onto the orthogonal standard-ordered unnormalized spin-adapted states mentioned above, and also use the unnormalized t matrix elements defined by (3.31), then we obtain the following system of coupled nonlinear algebraic equations for the orthogonally-spin-adapted t_1, t_2, and t_3 matrix elements:

$$\left\langle \begin{matrix} a^1 \\ a_1 \end{matrix} \right| \mathcal{H}_C^{(1)} \left| \ \Phi_0 \right\rangle = \sum_{j=0}^{3} \ \langle a^1|\Lambda^{1,j}| \ a_1\rangle = 0 , \quad (4.2a)$$

$$N_a^{-1}\left\langle \tilde{S}_i \begin{matrix} a^1 a^2 \\ a_1 a_2 \end{matrix} \right| \mathcal{H}_C^{(2)} \left| \ \Phi_0 \right\rangle$$

$$= \sum_{j=0}^{3} \ \langle a^1 a^2| \ \Lambda^{2,j} (\tilde{S}_i)| \ a_1 a_2\rangle = 0 , \quad (4.2b)$$

$$N_a^{-1}\left\langle \tilde{S} \begin{matrix} a^1 a^2 a^3 \\ a_1 a_2 a_3 \end{matrix} \right| \mathcal{H}_C^{(3)} \left| \ \Phi_0 \right\rangle$$

$$= \sum_{j=2}^{3} \ \langle a^1 a^2 a^3| \ \Lambda^{3,j} (\tilde{S})| \ a_1 a_2 a_3\rangle = 0, \quad (4.2c)$$

and the equation

$$\langle \Phi_0| \ \mathcal{H}_C^{(0)} | \ \Phi_0\rangle = \sum_{j=1}^{2} \ \Lambda^{0,j} = \Delta\epsilon^{(1)} + \Delta\epsilon^{(2)} = \Delta\epsilon , \quad (4.3)$$

which determines the correlation energy in terms of the t_1 and t_2 matrix elements. Except for the case $i = j = 2$ the terms $\Lambda^{i,j}$, $j \geq 1$, in (4.2) are linear in the t_j matrix elements, and are obtained from the connected resulting diagrams having i open paths, formed from one H skeleton and one M skeleton consisting of a single T_j skeleton (T skeleton having j open paths).[10] The inhomogeneous terms are those in (4.2a) and (4.2b) with $j = 0$. In the HF case the linear part of $\Lambda^{0,1}$ and the inhomogeneous term $\Lambda^{1,0}$ do not contribute. For $i = j = 2$, both the linear terms $\Lambda_L^{2,2}$ in the t_2 matrix elements and the nonlinear terms $\Lambda_{NL}^{2,2}$ (M skeleton consisting of two T_2 skeletons), arising from the disconnected tetraexcited cluster component $\frac{1}{2}T_2^2$, occur. Thus,

$$\Lambda^{2,2} = \Lambda_L^{2,2} + \Lambda_{NL}^{2,2} . \quad (4.4)$$

The CPMET approximation is obtained by considering only the terms $\Lambda^{2,0}$ and $\Lambda^{2,2}$ in (4.2b) and the terms $\Lambda^{0,2}$ in (4.3).

The orbital and spin diagrams for the two terms in (4.4) and the inhomogeneous term $\Lambda^{0,2}$ are given in Figs. 3 and 5 of Ref. 1 and the orbital diagrams for (4.3) are given in Fig. 13 of Ref. 1. The orbital diagrams for the terms $\Lambda^{1,1}$ are essentially the same as those given in Fig. 3 of Ref. 11. The corresponding spin diagrams are trivial and are easily obtained from the graphical representation of the monoexcited states given in Fig. 2 of Ref. 4. In a similar manner the orbital and spin diagrams for the terms $\Lambda^{1,2}$ and $\Lambda^{2,1}$ are easily obtained from the graphical representations in Fig. 4 of Ref. 1.

In the present paper we give only the orbital diagrams for $\Lambda^{1,3}$, $\Lambda^{2,3}$, $\Lambda^{3,2}$, and $\Lambda^{3,3}$ in Figs. 3 and 4, respectively.[29] The external-line particle and hole labels in Figs. 3 and 4 correspond to those appearing in the states of (4.2), and are assigned in all distinct ways using $\kappa, \lambda = 1, 2$ ($\bar{1} = 2$, $\bar{2} = 1$) for the biexcited-state orbital indices and $\kappa, \lambda = 1, 2, 3$; $\tau, \mu = 1, 2$ for triexcited-state orbital indices (cf. Sec. III). Thus, for example, Fig. 3(c), parts (i)
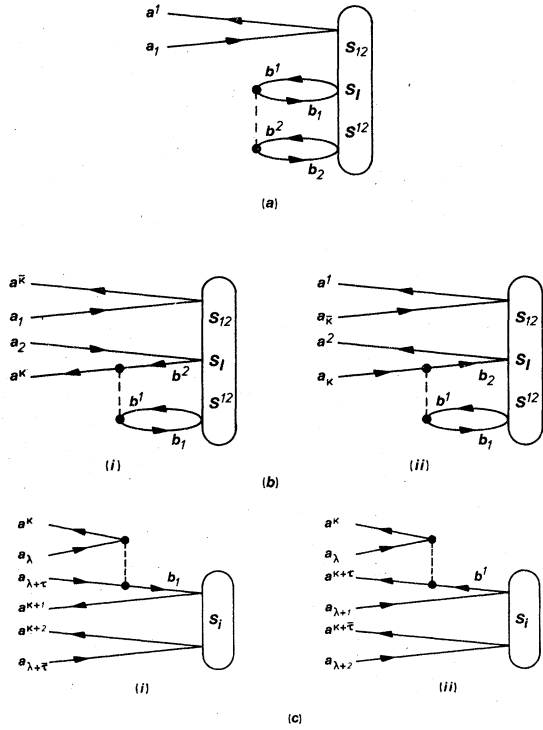
FIG. 3. Brandow form of orbital Goldstone-Hugenholtz diagrams associated with the terms $\Lambda^{1,3}$ (a), $\Lambda^{2,3}$ (b), and $\Lambda^{3,2}$ (c) appearing in Eqs. (4.5d), (4.6e), and (4.7a) (cf. text for details). The spin labels within the ovals representing the Brandow t vertices are those associated with the corresponding t_2 or t_3 matrix elements [cf. Eqs. (3.28)].

FIG. 4. Brandow form of orbital Goldstone-Hugenholtz diagrams associated with the terms $\Lambda^{3,3}$ in Eq. (4.7b) (cf. caption to Fig. 3).

and (ii) each represent 18 diagrams, Fig. 4(a), parts (i) and (ii) and Fig. 4(b), parts (i) and (ii) each represent three diagrams and Figs. 4(c) and 4(d) each represent nine diagrams. In labeling the external lines we recall that a Brandow t vertex is really a Hugenholtz vertex expressed as one of its representative Goldstone versions[1, 24] and hence, for example, since the three external hole lines in Fig. 4(a), part (i) are all equivalent, they can be labeled in only one way. On the other hand, since only the top two external hole lines in Fig. 4(b), part (ii) are equivalent, the hole lines can be labeled in three distinct ways. Finally, in Fig. 3(c), part (ii) the three hole lines are inequivalent and the bottom two particle lines are equivalent so we obtain $6 \times 3 = 18$ distinct labeling schemes for the external lines.

The weight factors[23] for the orbital diagrams of Figs. 3 and 4 are all unity, except for Fig. 3(a), which has a weight factor of $\frac{1}{2}$. The sign factors are easily determined from the $(-1)^{l+h+p}$ rule [cf. Eq. (37) of Ref. 1].[30]

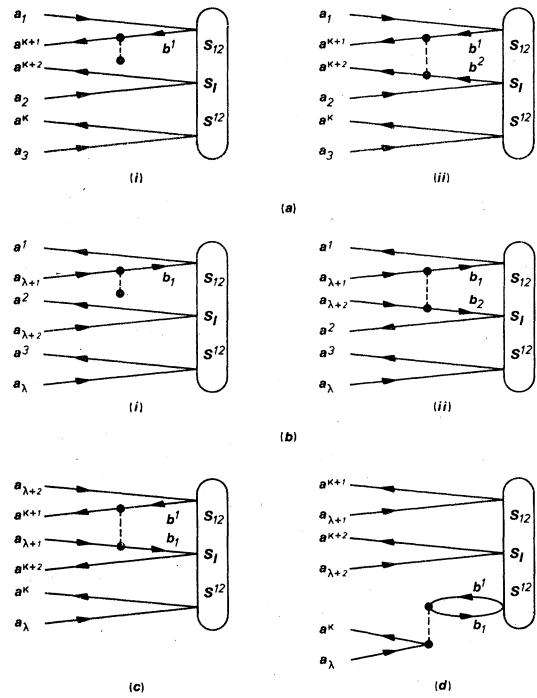The spin diagrams for Figs. 3 and 4 are given in

Figs. 5 and 6, respectively, where, for example, Fig. 4(a), parts (i) and (ii) correspond to the same spin diagram, Fig. 6(a). We have used the labels $\kappa, \lambda, \tau, \mu$ where necessary, on the lines carrying spin-$\frac{1}{2}$ to indicate how the lines are connected to-
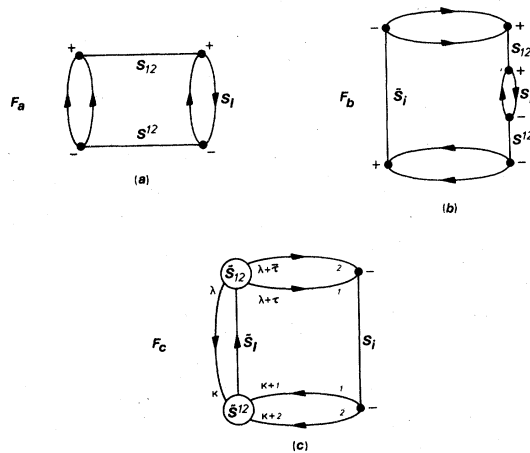
FIG. 5. Spin diagrams associated with the orbital diagrams of Fig. 3. (a), (b), and (c) correspond to Figs. 3 (a), 3 (b), parts (i) and (ii), and 3 (c), parts (i) and (ii), respectively. The overall factors are $F_a = 2^{-1/2} F$, $F_b = (-1)^{R(1+S_i)}[S_i]^{1/2} F$, and $F_c = [S_i]^{1/2} \tilde{F}$, where F and $\tilde{F}$ are defined in Fig. 1.
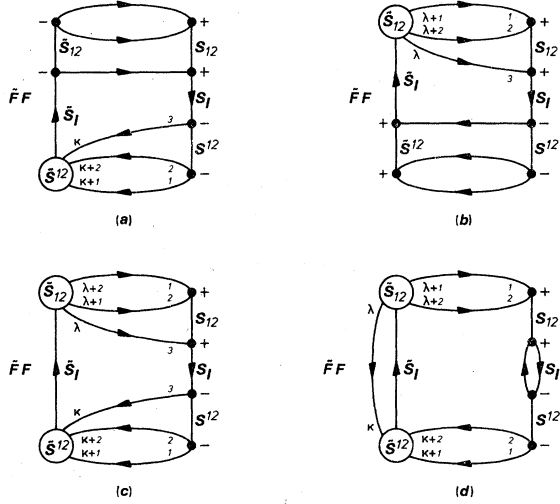
FIG. 6. Spin diagrams associated with the orbital diagrams of Fig. 4. (a), (b), (c), and (d) correspond to Figs. 4(a), parts (i) and (ii), 4(b), parts (i) and (ii), 4(c), and 4(d), respectively. The overall factor for each diagram is $\tilde{F}F$, where F and $\tilde{F}$ are defined in Fig. 1.

gether, using the compact graphical representation of Fig. 1(d). The spin diagrams are easily evaluated using the graphical rules given in Appendix I of Ref. 4. In particular, all spin diagrams can be separated across two lines using rule (70),[4] except for those in Figs. 5(c) and 6(d) which must be separated across three lines using rule (71).[4] Each smaller resulting diagram either reduces to oyster diagrams [cf. Eq. (74) of Ref. 4] by further separations across two lines, or to diagrams each representing a 6-j symbol [cf. Eq. (75) of Ref. 4]. Finally, the resulting spin coefficients and orbital factors which give the total contributions to the various $\Lambda^{i,j}$ terms, when multiplied together and summed over all orbital labels on internal lines and intermediate spin quantum numbers specified by the Brandow t vertices (untilded labels), are given in Tables IV and V.

Thus, we obtain the following expressions for the terms of the spin-adapted ECPMET equations (4.2):

$$\langle a^1 | \Lambda^{1,0} | a_1 \rangle = \sqrt{2} \, \langle a^1 | f | a_1 \rangle , \tag{4.5a}$$

$$\langle a^1 | \Lambda^{1,1} | a_1 \rangle = \sum_{b^1} \langle a^1 | f | b^1 \rangle \langle b^1 | t_1(0) | a_1 \rangle - \sum_{b_1} \langle b_1 | f | a_1 \rangle \langle a^1 | t_1(0) | b_1 \rangle$$

$$+ \sum_{b^1 b_1} (2 \langle a^1 b_1 | v | a_1 b^1 \rangle - \langle a^1 b_1 | v | b^1 a_1 \rangle) \langle b^1 | t_1(0) | b_1 \rangle , \tag{4.5b}$$

$$\langle a^1 | \Lambda^{1,2} | a_1 \rangle = \sum_{S_i} \sum_{b^1 b_1} (-1)^{S_i} (\tfrac{1}{2}[S_i])^{1/2}$$

$$\times \left(\sum_{b_2} \langle b_1 b_2 | v | b^1 a_1 \rangle \langle b^1 a^1 | \tau_2(S_i) | b_1 b_2 \rangle - \sum_{b^2} \langle a^1 b_1 | v | b^2 b^1 \rangle \langle b^1 b^2 | \tau_2(S_i) | b_1 a_1 \rangle \right), \tag{4.5c}$$

$$\langle a^1 | \Lambda^{1,3} | a_1 \rangle = 2^{-3/2} \sum_{S_{12}, S_I} [S_I]^{1/2} \sum_{b^1 b^2} \sum_{b_1 b_2} \langle b_1 b_2 | v | b^1 b^2 \rangle \langle a^1 b^1 b^2 | \tau_3(S_{12}, S_{12}, S_I) | a_1 b_1 b_2 \rangle ; \tag{4.5d}$$

$$\langle a^1 a^2 | \Lambda^{2,0}(\tilde{S}_i) | a_1 a_2 \rangle = -[\tilde{S}_i]^{1/2} \sum_{K=1}^{2} (-1)^{K \tilde{S}_i} \langle a^K a^{\bar{K}} | v | a_1 a_2 \rangle , \tag{4.6a}$$

TABLE IV. Contributions of the orbital diagrams (Fig. 3) and the spin diagrams (Fig. 5) corresponding to the terms $\Lambda^{1,3}$, $\Lambda^{2,3}$, and $\Lambda^{3,2}$ of the ECPMET equations.

Orbital diagram	Weight factor	Orbital factor $\mathcal{S} = \{S_{12}, S^{12}, S_I\}$	Spin diagram	Spin factor
(a)	$\tfrac{1}{2}$	$\langle b_1 b_2 | v | b^1 b^2 \rangle \langle a^1 b^1 b^2 | \tau_3(\mathcal{S}) | a_1 b_1 b_2 \rangle$	(a)	$(\tfrac{1}{2}[S_I])^{1/2} \delta(S_{12}, S^{12})$
b(i)	1	$(-1)^K \langle a^K b_1 | v | b^2 b^1 \rangle \langle a^K b^2 b^1 | \tau_3(\mathcal{S}) | a_1 a_2 b_1 \rangle$	(b)	$(-1)^{\bar{K}(1+\tilde{S}_i)} \chi [S_I]/[\tilde{S}_i])^{1/2}$
b(ii)	1	$(-1)^{\bar{K}} \langle b_2 b_1 | v | a_K b^1 \rangle \langle a^1 a^2 b^1 | \tau_3(\mathcal{S}) | a_{\bar{K}} b_2 b_1 \rangle$		$\times \delta(\tilde{S}_i, S_{12}) \delta(\tilde{S}_i, S^{12})$
c(i)	1	$(-1)^\tau \langle a^K b_1 | v | a_\lambda a_{\lambda+\tau} \rangle \langle a^{K+1} a^{K+2} | \tau_2(S_i) | b_1 a_{\lambda+\bar\tau} \rangle$	(c)	$(-1)^{\tau(1+S_i)} ([\tilde{S}_I]/[S_I])^{1/2}$
c(ii)	1	$(-1)^{\bar\tau} \langle a^K a^{K+\tau} | v | a_\lambda b^1 \rangle \langle b^1 a^{K+\bar\tau} | \tau_2(S_i) | a_{\lambda+1} a_{\lambda+2} \rangle$		$\times D_K(\tilde{S}_I; \tilde{S}^{12}, S_i) D_\lambda(\tilde{S}_I; \tilde{S}_{12}, S_i)$

TABLE V. Contributions of the orbital diagrams (Fig. 4) and the spin diagrams (Fig. 6) corresponding to the term $\Lambda^{3,3}$ of the ECPMET equations.

Orbital diagram	Weight factor	Orbital factor $\mathcal{S} = \{S_{12}, S^{12}, S_I\}$	Spin diagram	Spin factor
a(i)	1	$\langle a^{\kappa+1}|f|b^1\rangle \langle b^1 a^{\kappa+2} a^\kappa | \tau_3(\mathcal{S})|a_1 a_2 a_3\rangle$		$\delta(\tilde{S}_I, S_I)\delta(\tilde{S}_{12}, S_{12})$
a(ii)	1	$\langle a^{\kappa+1} a^{\kappa+2}|v|b^1 b^2\rangle \langle b^1 b^2 a^\kappa | \tau_3(\mathcal{S})|a_1 a_2 a_3\rangle$	(a)	$\times D_\kappa(\tilde{S}_I; \tilde{S}^{12}, S^{12})$
b(i)	1	$-\langle b_1|f|a_{\lambda+1}\rangle \langle a^1 a^2 a^3 | \tau_3(\mathcal{S})|b_1 a_{\lambda+2} a_\lambda\rangle$		$\delta(\tilde{S}_I, S_I)\delta(\tilde{S}^{12}, S^{12})$
b(ii)	1	$\langle b_1 b_2|v|a_{\lambda+1} a_{\lambda+2}\rangle \langle a^1 a^2 a^3 | \tau_3(\mathcal{S})|b_1 b_2 a_\lambda\rangle$	(b)	$\times D_\lambda(\tilde{S}_I; \tilde{S}_{12}, S_{12})$
(c)	1	$\langle a^{\kappa+1} b_1|v|b^1 a_{\lambda+1}\rangle \langle b^1 a^{\kappa+2} a^\kappa | \tau_3(\mathcal{S})|a_{\lambda+2} b_1 a_\lambda\rangle$	(c)	$(-1)^{1+S_{12}}\delta(\tilde{S}_I, S_I)$
				$\times D_\kappa(\tilde{S}_I; \tilde{S}^{12}, S^{12})D_\lambda(\tilde{S}_I; \tilde{S}_{12}, S_{12})$
(d)	1	$\langle a^\kappa b_1|v|a_\lambda b^1\rangle \langle a^{\kappa+1} a^{\kappa+2} b^1 | \tau_3(\mathcal{S})|a_{\lambda+1} a_{\lambda+2} b_1\rangle$	(d)	$[\tilde{S}_I, S_I]^{1/2}[S_{12}]^{-1}\delta(S^{12}, S_{12})$
				$\times D_\kappa(\tilde{S}_I; \tilde{S}^{12}, S_{12})D_\lambda(\tilde{S}_I; \tilde{S}_{12}, S_{12})$

$$\langle a^1 a^2| \Lambda^{2,1}(\tilde{S}_i)| a_1 a_2\rangle = (\tfrac{1}{2}[\tilde{S}_i])^{1/2} \sum_{\kappa,\lambda=1}^{2} (-1)^{(\kappa+\lambda+1)\tilde{S}_i}$$

$$\times \left(\sum_{b^1} \langle b_1 a^{\bar{\kappa}}|v| a_\lambda a_{\bar{\lambda}}\rangle \langle a^\kappa| t_1(0)| b_1\rangle - \sum_{b^1} \langle a^\lambda a^{\bar{\lambda}}|v| b^1 a_{\bar{\kappa}}\rangle \langle b^1| t_1(0)| a_\kappa\rangle \right), \tag{4.6b}$$

$$\langle a^1 a^2| \Lambda^{2,2}_L(\tilde{S}_i)| a_1 a_2\rangle = \sum_{\kappa=1}^{2} \left(\sum_{b^1} \langle a^\kappa|f| b^1\rangle \langle b^1 a^{\bar{\kappa}}| \tau_2(\tilde{S}_i)| a_\kappa a_{\bar{\kappa}}\rangle - \sum_{b_1} \langle b_1|f| a_\kappa\rangle \langle a^\kappa a^{\bar{\kappa}}| \tau_2(\tilde{S}_i)| b_1 a_{\bar{\kappa}}\rangle \right)$$

$$+ \sum_{b^1 b^2} \langle a^1 a^2| v| b^1 b^2\rangle \langle b^1 b^2| \tau_2(\tilde{S}_i)| a_1 a_2\rangle + \sum_{b_1 b_2} \langle b_1 b_2|v| a_1 a_2\rangle \langle a^1 a^2| \tau_2(\tilde{S}_i)b_1 b_2\rangle$$

$$+\frac{1}{2} \sum_{\kappa,\lambda=1}^{2} \sum_{S_i} \sum_{b^1 b_1} (-1)^{(\kappa+\lambda)\tilde{S}_i} \left([\tilde{S}_i, S_i]^{1/2}\langle a^\kappa b_1|v| a_{\bar{\lambda}} b^1\rangle \right.$$

$$\left. - 2\delta(\tilde{S}_i, S_i)\langle a^\kappa b_1|v| b^1 a_{\bar{\lambda}}\rangle \right) \langle b^1 a^{\bar{\kappa}}| \tau_2(S_i)| a_\lambda b_1\rangle, \tag{4.6c}$$

$$\langle a^1 a^2| \Lambda^{2,2}_{NL}(\tilde{S}_i)| a_1 a_2\rangle = \sum_{\kappa=1}^{2} \sum_{S_i^1 S_i^2} \sum_{b^1 b^2} \sum_{b_1 b_2} (-1)^{\kappa\tilde{S}_i + S_i^1 + S_i^2}[\tilde{S}_i, S_i^1, S_i^2]^{1/2}$$

$$\times [C(\tilde{S}_i, S_i^1, S_i^2)\langle b_1 b_2|v| b^2 b^1\rangle - \tfrac{1}{4}\langle b_1 b_2|v| b^1 b^2\rangle]\langle a^1 b^1| \tau_2(S_i^1)| a_\kappa b_1\rangle \langle a^2 b^2| \tau_2(S_i^2)| a_{\bar{\kappa}} b_2\rangle$$

$$+\frac{1}{2} \sum_{\kappa=1}^{2} \sum_{S_i} \sum_{b^1 b^2} \sum_{b_1 b_2} (-1)^{\kappa\tilde{S}_i}[S_i]^{1/2}\langle b_1 b_2|v| b^1 b^2\rangle$$

$$\times [\langle a^1 a^2| \tau_2(\tilde{S}_i)| a_{\bar{\kappa}} b_2\rangle \langle b^1 b^2| \tau_2(S_i)| a_\kappa b_1\rangle + \langle b^2 a^\kappa| \tau_2(\tilde{S}_i)|a_1 a_2\rangle \langle a^{\bar{\kappa}} b^1| \tau_2(S_i)| b_1 b_2\rangle]$$

$$-\tfrac{1}{2}(-1)^{\tilde{S}_i}[\tilde{S}_i]^{-1/2} \sum_{b^1 b^2} \sum_{b_1 b_2} \langle b_1 b_2|v| b^1 b^2\rangle \langle b^1 b^2| \tau_2(\tilde{S}_i)|a_1 a_2\rangle \langle a^1 a^2| \tau_2(\tilde{S}_i)| b_1 b_2\rangle, \tag{4.6d}$$

$$\langle a^1 a^2|\Lambda^{2,3}(\tilde{S}_i)|a_1 a_2\rangle = \sum_{\kappa=1}^{2} \sum_{S} \sum_{b^1 b_1} (-1)^{\bar{\kappa}\tilde{S}_i}\left(\frac{[S_I]}{[\tilde{S}_i]} \right)^{1/2} \delta(S_{12}, \tilde{S}_i)\delta(S^{12}, \tilde{S}_i)$$

$$\times \left(\sum_{b_2} \langle b_2 b_1|v| a_\kappa b^1\rangle \langle a^1 a^2 b^1| \tau_3(\mathcal{S})| a_{\bar{\kappa}} b_2 b_1\rangle - \sum_{b^2} \langle a^\kappa b_1|v|b^2 b^1\rangle \langle a^{\bar{\kappa}} b^2 b^1| \tau_3(\mathcal{S})| a_1 a_2 b_1\rangle \right); \tag{4.6e}$$

$$\langle a^1 a^2 a^3 | \Lambda^{3,\,2}(\tilde{S}) | a_1 a_2 a_3 \rangle = \sum_{\kappa,\lambda=1}^{3} \sum_{\tau=1}^{2} \sum_{S_i} (-1)^{\tau S_i} \left(\frac{[\tilde{S}_I]}{[S_i]} \right)^{1/2} D_\kappa(\tilde{S}_I; \tilde{S}^{12}, S_i) D_\lambda(\tilde{S}_I; \tilde{S}_{12}, S_i)$$

$$\times \left(\sum_{b_1} \langle a^\kappa b_1 | v | a_\lambda a_{\lambda+\tau} \rangle \langle a^{\kappa+1} a^{\kappa+2} | \tau_2(S_i) | b_1 a_{\lambda+\bar\tau} \rangle \right.$$

$$\left. - \sum_{b_1} \langle a^\kappa a^{\kappa+\tau} | v | a_\lambda b^1 \rangle \langle b^1 a^{\kappa+\bar\tau} | \tau_2(S_i) | a_{\lambda+1} a_{\lambda+2} \rangle \right), \tag{4.7a}$$

$$\langle a^1 a^2 a^3 | \Lambda^{3,\,3}(\tilde{S}) | a_1 a_2 a_3 \rangle = \sum_{\kappa=1}^{3} \sum_{S} \delta(\tilde{S}_I, S_I) \delta(\tilde{S}_{12}, S_{12}) D_\kappa(\tilde{S}_I; \tilde{S}^{12}, S^{12})$$

$$\times \left(\sum_{b_1} \langle a^{\kappa+1} | f | b^1 \rangle \langle b^1 a^{\kappa+2} a^\kappa | \tau_3(S) | a_1 a_2 a_3 \rangle + \sum_{b_1 b_2} \langle a^{\kappa+1} a^{\kappa+2} | v | b^1 b^2 \rangle \langle b^1 b^2 a^\kappa | \tau_3(S) | a_1 a_2 a_3 \rangle \right)$$

$$+ \sum_{\lambda=1}^{3} \sum_{S} \delta(\tilde{S}_I, S_I) D_\lambda(\tilde{S}_I; \tilde{S}_{12}, S_{12}) \delta(\tilde{S}^{12}, S^{12})$$

$$\times \left(-\sum_{b_1} \langle b_1 | f | a_{\lambda+1} \rangle \langle a^1 a^2 a^3 | \tau_3(S) | b_1 a_{\lambda+2} a_\lambda \rangle \right.$$

$$\left. + \sum_{b_1 b_2} \langle b_1 b_2 | v | a_{\lambda+1} a_{\lambda+2} \rangle \langle a^1 a^2 a^3 | \tau_3(S) | b_1 b_2 a_\lambda \rangle \right)$$

$$- \sum_{\kappa,\lambda=1}^{3} \sum_{S} \delta(\tilde{S}_I, S_I) D_\lambda(\tilde{S}_I; \tilde{S}_{12}, S_{12}) D_\kappa(\tilde{S}_I; \tilde{S}^{12}, S^{12})$$

$$\times \sum_{b_1 b_1} \langle a^{\kappa+1} b_1 | v | b^1 a_{\lambda+1} \rangle \langle b^1 a^{\kappa+2} a^\kappa | \tau_3(S) | b_1 a_{\lambda+2} a_\lambda \rangle$$

$$+ \sum_{\kappa,\lambda=1}^{3} \sum_{S} [\tilde{S}_I, S_I]^{1/2} [S_{12}]^{-1} \delta(S^{12}, S_{12}) D_\kappa(\tilde{S}_I; \tilde{S}^{12}, S_{12}) D_\lambda(\tilde{S}_I; \tilde{S}_{12}, S_{12})$$

$$\times \sum_{b_1 b_1} \langle a^\kappa b_1 | v | a_\lambda b^1 \rangle \langle a^{\kappa+1} a^{\kappa+2} b^1 | \tau_3(S) | a_{\lambda+1} a_{\lambda+2} b_1 \rangle . \tag{4.7b}$$

In these formulas we are using the notation introduced in (3.7) and (3.20), and the notation S $=\{ S_{12}, S^{12}, S_I \}$, $\tilde{S} =\{ \tilde{S}_{12}, \tilde{S}^{12}, \tilde{S}_I \}$ for the sets of intermediate spin quantum numbers which label the t_3 matrix elements and the triexcited states onto which the Schrödinger equation is projected, respectively. The spin coefficient C appearing in (4.6d) is a 9-j symbol defined by [cf. Eq. (43) of Ref. 1]

$$C(X_1, X_2, X_3) = \begin{Bmatrix} X_1 & \frac{1}{2} & \frac{1}{2} \\ \frac{1}{2} & X_2 & \frac{1}{2} \\ \frac{1}{2} & \frac{1}{2} & X_3 \end{Bmatrix}, \tag{4.8}$$

and satisfies

$$C(X_i, X_j, X_k) = C(X_1, X_2, X_3) \tag{4.9}$$

for any permutation of the indices. The explicit values for $X_i = 0, 1$ are given in Table VI. The spin coefficients D appearing in (4.7) are defined

in Table I (cf. Sec. III).

The contributions to the correlation energy in (4.3) are easily determined from the diagrams of Figs. 10(i) and 13 of Ref. 1. Thus,

$$\Delta\epsilon^{(1)} = \sqrt{2} \sum_{b_1 b_1} \langle b_1 | f | b^1 \rangle \langle b^1 | t_1(0) | b_1 \rangle$$

$$+ \frac{1}{2} \sum_{b_1 b_2} \sum_{b_1 b_2} (2 \langle b_1 b_2 | v | b^1 b^2 \rangle$$

$$- \langle b_1 b_2 | v | b^2 b^1 \rangle) \langle b^1 | t_1(0) | b_1 \rangle \langle b^2 | t_1(0) | b_2 \rangle \tag{4.10a}$$

and

$$\Delta\epsilon^{(2)} = \frac{1}{2} \sum_{S_i} \sum_{b_1 b_2} \sum_{b_1 b_2} (-1)^{1+S_i} [S_i]^{1/2}$$

$$\times \langle b_1 b_2 | v | b^1 b^2 \rangle \langle b^1 b^2 | \tau_2(S_i) | b_1 b_2 \rangle . \tag{4.10b}$$

TABLE VI. Spin coefficient (9-j symbol) defined in Eq. (4.8).

X_1	X_2	X_3	$C(X_1,X_2,X_3)$
0	0	0	$-\frac{1}{4}$
1	0	0	$\frac{1}{4}$
1	1	0	$\frac{1}{12}$
1	1	1	$\frac{5}{36}$

The first term in (4.10a) vanishes in the HF case, while the second term, which first appears in the third order of perturbation theory, is usually negligible in comparison with $\Delta\epsilon^{(2)}$, which first appears in the second order.

V. DISCUSSION

The orthogonally-spin-adapted equations, which are given in Sec. IV, represent a simple and symmetric form of the ECPMET equations for the minimal number of t matrix elements. Also, because of the orthogonality of our states, the matrices corresponding to the linear and nonlinear parts of the ECPMET equations are sparser than in the nonorthogonal case (cf. Sec. I). The spin coefficients which are needed in the orthogonal case are quite simple: the only nontrivial spin coefficients are a simple 6-j symbol [Eq. (3.19) and Tables I and II] needed for the triexcited part, and a simple 9-j symbol [Eq. (4.8) and Table VI] needed for the nonlinear part.

The ECPMET equations, that have been given here in terms of unnormalized states and t matrix elements, can easily be converted to equations involving normalized states and t matrix elements by (i) using Eqs. (3.31) to replace unnormalized t_2 and t_3 matrix elements by normalized ones, (ii) multiplying Eqs. (4.2b) and (4.2c) by the normalization factor N_a of the state onto which the Schrödinger equation is projected.

We can write the unnormalized form of the ECPMET equations in the compact form

$$a_i + \sum_{j=1}^{M} b_{ij}\,\tau_j + \sum_{j\leq k=1}^{N} c_{ijk}\,\tau_j\,\tau_k = 0, \quad (i=1,\ldots,M),$$

$$(5.1)$$

where M is the total number of monoexcited, biexcited and triexcited states, N is the total number of biexcited states, and τ_j is an unnormalized t matrix element. The coefficients a_i, b_{ij}, and c_{ijk} are given in Eqs. (4.5)–(4.7) in terms of the f and v matrix elements, and $a_i = 0$ if i designates a triexcited state or, in the HF case, a monoexcited state.

By applying steps (i) and (ii) above, we obtain the normalized set of equations

$$a_i' + \sum_{j=1}^{M} b_{ij}'\,t_j + \sum_{j\leq k=1}^{N} c_{ijk}'\,t_j\,t_k = 0$$

$$(i=1,\ldots,M), \quad (5.2)$$

where

$$a_i' = N_i\,a_i, \tag{5.3a}$$

$$b_{ij}' = N_i N_j^{-1} b_{ij}, \tag{5.3b}$$

$$c_{ijk}' = N_i\,(N_j N_k)^{-1} c_{ijk}. \tag{5.3c}$$

Here, N_i is the pertinent normalization factor, Eq. (3.11), and t_i is a normalized t-matrix element. We also note that the matrix representing the linear part of the CPMET equations becomes hermitian (symmetric in the real case) if normalized states and t matrix elements are used.

From Eqs. (5.2) and (5.3) we can easily obtain the formulas needed in the direct configuration (CI) method of Roos and Siegbahn (cf. Ref. 15). Using the notation of Refs. 4 and 15, such formulas are given in terms of the CI expansion coefficients c_j and the matrix elements of the Hamiltonian H_N, by

$$\Delta\sigma_i = \sum_{j=1}^{M} \langle i\,|\,H_N|\,j\,\rangle\,c_j. \tag{5.4}$$

Here, as in (5.1), i and j index the distinct monoexcited, biexcited and triexcited states. In most cases the diagrams that we have used to obtain the linear terms of the ECPMET equations (cf. for example, Figs. 3 and 4) can also be used to evaluate the matrix elements $\langle i\,|\,H_N|\,j\rangle$ in (5.4).[31] Thus from (5.2), we immediately obtain

$$\langle i\,|\,H_N|\,j\rangle = b_{ij}', \tag{5.5}$$

and the right-hand side of (5.4) can be written explicitly from the linear part of (5.2), after replacing t_j by the corresponding CI coefficient c_j, and using (5.3b) and the pertinent expressions from (4.5)–(4.7) for b_{ij}. We note, however, that
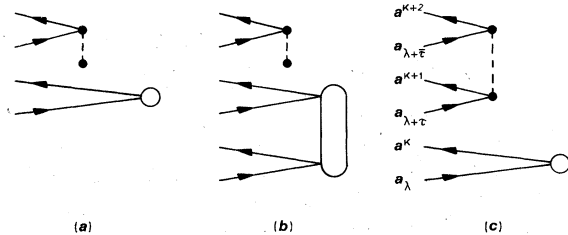

FIG. 7. Disconnected diagrams which appear in direct CI but not in ECPMET (cf. Sec. V for details).

some of the diagrams needed for the evaluation of the matrix elements of H_N in (5.5) may correspond to disconnected diagrams of ECPMET which, of course, do not appear in the final form of the coupled-cluster theory. Thus, in such cases, the right-hand side of (5.5) will also contain a term b''_{ij} arising from such disconnected diagrams:

$$\langle i \mid H_N \mid j \rangle = b'_{ij} + b''_{ij} \ . \tag{5.6}$$

If only monoexcited, biexcited, and triexcited states are considered, then it is easily seen that $b''_{ij} \neq 0$ only for the disconnected diagrams shown in Fig. 7. In the HF case, which we are considering, only the diagram in Fig. 7(c) will contribute. In fact, this diagram gives directly the contribution to (5.4) when i designates a triexcited state and j is summed over the monoexcited states, since no connected diagrams are possible in this case [cf. Eq. (4.2c)]. Thus, using the notation introduced in (4.2), and denoting a general monoexcited CI coefficient by $\langle b^1 \mid c_1 \mid b_1 \rangle$, we obtain the contribution

$$\langle a^1 a^2 a^3 \mid \Lambda_D^{3;1} (\tilde{S}) \mid a_1 a_2 a_3 \rangle = N_a (\tfrac{1}{2} [\tilde{S}_I])^{1/2} \sum_{\kappa, \lambda=1}^{3} \sum_{\tau=1}^{2} (-1)^{\overline{\tau S}} \, {}_{12}D_{2\kappa+\lambda} (\tilde{S}_I; \tilde{S}^{12}, \tilde{S}_{12}) \langle a^{\kappa+1} a^{\kappa+2} \mid v \mid a_{\lambda+\tau} a_{\lambda+\overline{\tau}} \rangle \langle a^{\kappa} \mid c_1 \mid a_{\lambda} \rangle \tag{5.7}$$

from the diagram in Fig. 7(c). Here, the subscript D is used to emphasize that this is a disconnected contribution and hence does not appear in the ECPMET equation, (4.2c).

Thus, in the HF case we can obtain the direct CI formulas, involving orthogonally-spin-adapted monoexcited, biexcited, and triexcited states, directly from the linear part of the ECPMET equations, (4.5)–(4.7), except for the term given in (5.7). For the case of biexcited direct CI, we have previously obtained compact expressions for Eq. (5.4) directly from formulas for the matrix elements of the Hamiltonian between orthogonally-spin-adapted pp-hh–coupled spin-adapted states [cf. Eqs. (49) of Ref. 4]. On the other hand, we can use the expression that we have obtained in the present paper for the right-hand side of (5.6) to derive compact expressions for the matrix elements of the Hamiltonian between orthogonally-spin-adapted monoexcited, biexcited and triexcited states.[32]

ACKNOWLEDGMENTS

*Also at Guelph-Waterloo Center for Graduate Work in Chemistry and Chemistry Dept., Univ. of Waterloo, Waterloo, Ontario, Canada.

[1] J. Paldus, J. Chem. Phys. 67, 303 (1977).

[2] We are using the graphical methods of Ref. 3. A useful summary is presented in Appendix I of Ref. 4. Other approaches are given in Ref. 5, where only the 3-jm symbols are represented graphically, Ref. 6 where only the CG coefficients are represented, and Refs. 7 and 8, where both CG and 3-jm coefficients are represented. A review of the latter approach, with applications, is also given in Ref. 9.

[3] E. El Baz and B. Castel, *Graphical Methods of Spin Algebras in Atomic, Nuclear, and Particle Physics* (Marcel Dekker, New York, 1972).

[4] J. Paldus, B. G. Adams, and J. Čížek, Int. J. Quantum Chem. 11, 813 (1977).

[5] A. P. Jucys, I. B. Levinson, and V. V. Vanagas, *Mathematical Apparatus of the Theory of Angular Momentum* (Institute of Physics and Mathematics of the Academy of Sciences of the Lithuanian S. S. R., Mintis,

Vilnius, 1960), in Russian (English translations by Israel Program for Scientific Translations, Jerusalem, 1962, and Gordon and Breach, New York, 1964).

[6] A. P. Jucys and A. A. Bandzaitis, *The Theory of Angular Momentum in Quantum Mechanics*, 2nd ed. (Mokslas, Vilnius, Lithuania, 1977), in Russian.

[7] I. Lindgren and J. Morrison, *Atomic Many-Body Theory* (Springer Verlag, Berlin, to be published).

[8] D. M. Brink and G. R. Satchler, *Angular Momentum*, 2nd ed. (Clarendon, Oxford, 1968).

[9] P. G. H. Sandars, in *Atomic Physics and Astrophysics*, Brandeis University Summer Institute in Theoretical Physics, 1969, Vol. 1, edited by M. Chrétien and E. Lipworth (Gordon and Breach, New York, 1971), p. 171.

[10] J. Čížek, J. Chem. Phys. 45, 4256 (1966); Adv. Chem. Phys. 14, 35 (1969).

[11] J. Paldus, J. Čížek, and I. Shavitt, Phys. Rev. A 5, 50 (1972).

[12] In Ref. 1 this form of the coupled cluster theory was simply referred to as the spin adapted form and the

orbital formalism of Refs. 10 and 11 was referred to as the spin nonadapted form. This terminology is imprecise for even the orbital form of the coupled-cluster theory is spin adapted, since the clusters considered are pure singlets. However, it is derived by projecting the Schrödinger equation onto a *nonorthogonal* set of spin-bonded singlet functions, in contrast to the spin-adapted approach of Ref. 1, which is derived from *orthogonal* projections. Thus, we shall use the terminology "orthogonally spin adapted" and "nonorthogonally spin adapted" to distinguish these two formalisms.

[13] In the biexcited case the spin-bonded functions in the nonorthogonally-spin-adapted approach are $(a_1 a^p)(a_2 a^q)$, where (p, q) are the permutations $(1, 2)$ and $(2, 1)$. Thus, both functions are linearly independent although nonorthogonal. In the triexcited case the spin-bonded functions are $(a_1 a^p)(a_2 a^q)(a_3 a^r)$, where (p, q, r) is one of the $3! = 6$ permutations of $(1, 2, 3)$. Clearly these functions are linearly dependent. Defining the orbital sequence corresponding to the identity permutation as the standard one, we see easily that the permutation $(2, 3, 1)$ yields a nonstandard bracketing scheme [cf. I. Shavitt, in *Methods of Electronic Structure Theory*, edited by H. F. Schaefer, III (Plenum, New York, 1977)].

[14] See, for example, J. Flores and M. Moshinsky, Nucl. Phys. **A93**, 81 (1967); M. Moshinsky and T. H. Seligman, Ann. Phys. (N.Y.) **66**, 311 (1971); J. Paldus, in *Group Theoretical Methods in Physics, Proceedings, Austin 1978*, edited by W. Beiglboeck, A. Bohm, and E. Takasugi (Springer-Verlag, New York, to be published).

[15] B. Roos, Chem. Phys. Lett. **15**, 153 (1972); B. O. Roos and P. E. M. Siegbahn, in *Methods of Electronic Structure Theory*, edited by H. F. Schaefer, III (Plenum, New York, 1977), p. 277.

[16] B. G. Adams, Ph.D. thesis (University of Waterloo, 1978) (unpublished).

[17] J. Paldus, J. Čížek, M. Saute, and A. Laforgue, Phys. Rev. A **17**, 805 (1978).

[18] A. Pipano and I. Shavitt, Int. J. Quantum Chem. **2**, 741 (1968) (cf. also Ref. 11).

[19] R. P. Hosteny, R. R. Gilman, T. H. Dunning Jr., A. Pipano, and I. Shavitt, Chem. Phys. Lett. **7**, 325 (1970); C. W. Bauschlicher Jr. and I. Shavitt, J. Am.

Chem. Soc. **100**, 739 (1978); P. J. Hay and I. Shavitt, J. Chem. Phys. **60**, 2865 (1974); R. P. Hosteny, T. H. Dunning Jr., R. R. Gilman, A. Pipano, and I. Shavitt, *ibid.* **62**, 4764 (1975).

[20] B. R. Riemenschneider and N. R. Kestner, Chem. Phys. **3**, 193 (1974).

[21] W. Kutzelnigg, in *Methods of Electronic Structure Theory*, edited by H. F. Schaefer, III (Plenum, New York, 1977).

[22] K. Ruedenberg (private communication).

[23] J. Paldus and J. Čížek, Adv. Quantum Chem. **9**, 105 (1975).

[24] B. H. Brandow, Rev. Mod. Phys. **39**, 771 (1967).

[25] B. G. Adams, J. Paldus, and J. Čížek, Int. J. Quantum Chem. **11**, 849 (1977).

[26] J. Paldus, P. E. S. Wormer, Phys. Rev. A **18**, 827 (1978).

[27] It follows that our triexcited states will differ by at most a phase factor from the particle-hole Gelfand states for which a fixed ordering of orbitals is used, since any doubly occupied pair is coupled to zero spin.

[28] A. Messiah, *Quantum Mechanics*, Vol. 2 (Wiley, New York, 1966); cf. also Ref. 8.

[29] We have omitted several diagrams that vanish in the Hartree-Fock case since they contain matrix elements of the type $\langle b^1 | f | b_1 \rangle$.

[30] Here l is the number of closed loops of particle and hole lines, h is the number of the internal hole lines, and p is the parity of the permutation, which converts noncanonical open loop labeling schemes to canonical ones (Ref. 1) [in Fig. 3(b), part (i), $\kappa = 2$ gives the canonical labeling and hence $(-1)^p = (-1)^\kappa$].

[31] In Ref. 4 closed Goldstone diagrams were employed in the graphical representation of matrix elements of the Hamiltonian. The connection between these diagrams and the open Goldstone-Hugenholtz diagrams used in the coupled-cluster theory is easily obtained by comparing, for example, Fig. 8 (a) of Ref. 4 with Fig. 3(b), part (vi) of Ref. 1. Thus, if the "bra" state parts of the four diagrams of Fig. 8 (a) are removed then these diagrams correspond to the single diagram of Fig. 3 (b), part (vi).

[32] In Ref. 4 we have only considered matrix elements of the Hamiltonian involving monoexcited and biexcited states.